# Electronic Structure and Effectively Unpaired Electron Density Topology in *closo*-Boranes: Nonclassical Three-Center Two-Electron Bonding

Rosana M. Lobayan,[†] Roberto C. Bochicchio,*[,‡] Alicia Torre,[§] and Luis Lain[§]

[†]Facultad de Ingeniería, Universidad de la Cuenca del Plata, Lavalle 50, 3400, Corrientes, Argentina

[‡]Departamento de Física, Facultad de Ciencias Exactas y Naturales, Universidad de Buenos Aires, and Instituto de Física de Buenos Aires, Consejo Nacional de Investigaciones Científicas y Técnicas, Ciudad Universitaria, 1428, Buenos Aires, Argentina

[§]Departamento de Química Física, Facultad de Ciencia y Tecnología, Universidad del País Vasco, Apartado 644, E-48080 Bilbao, Spain

**ABSTRACT:** This article provides a detailed study of the structure and bonding in *closo*-borane cluster compounds $X_2B_3H_3$ (X = BH$^-$, P, SiH, CH, N), with particular emphasis on the description of the electron distribution using the topology of the quantum many-body effectively unpaired density. The close relationship observed between the critical points of this quantity and the localization of the electron cloud allows us to characterize the nonclassical bonding patterns of these systems. The obtained results confirm the suitability of the local rule to detect three-center two-electron bonds, which was conjectured in our previous study on boron hydrides.

## 1. INTRODUCTION

The physical information contained in *N*-electron molecular state functions is usually summarized by means of chemical descriptors which quantify the fundamental chemical concepts, such as atomic and bonding populations, bond orders and ionicities (bond multiplicities), atomic and free valencies, and others.[1−12] The electron density expressed as electron population[13−16] constitutes a tool of paramount importance in the treatments known as *nonlocal* or *integrated formulations*.[4,13−16] Complementary to these methodologies are those based on the study of the electron density $\rho(\mathbf{r})$ and its associated Laplacian field $\nabla^2\rho(\mathbf{r})$ through their topological structures, i.e., the localization and classification of their critical points (cp's), (i.e., maxima, minima, or saddle ones). This approach to interpret chemical information from the local point of view[17−19] will be called *local formulation*. A more detailed description of these methods of study may be found in ref 20.

An exact partitioning of the electron density has been reported so that $\rho(\mathbf{r}) = \rho^{(p)}(\mathbf{r}) + \rho^{(u)}(\mathbf{r})$ in which the contributions $\rho^{(p)}(\mathbf{r})$ and $\rho^{(u)}(\mathbf{r})$, possessing different physical characters, correspond to the effectively paired electron density and unpaired electron density, respectively.[21] Both contributions to the electron density have been topologically described by the localization of their critical points, the spatial shifts of these cp's in comparison with those of the total density, and the determination of the domains in which these scalar fields concentrate/reduce.[21,22]

It has been shown that the positions of the nuclear cp's (ncp's) (local maxima placed at the nuclear positions) of $\rho^{(p)}(\mathbf{r})$ are located very close to the total $\rho(\mathbf{r})$ ncp's, while those of $\rho^{(u)}(\mathbf{r})$ are also located close to the nuclear positions but out of the bonding region.[21] Further studies dealing with the utilization of the Laplacian functions $\nabla^2\rho^{(p)}(\mathbf{r})$ and $\nabla^2\rho^{(u)}(\mathbf{r})$ stressed the fact that nuclear regions possess most of the effectively unpaired electrons. Moreover, both paired and unpaired density fields possess successive regions of concentration and depletion of density, yielding a shell structure.[22] These mentioned results have been obtained from the application of this local formalism to systems possessing conventional patterns of bonding.[21,22] Recently, this treatment has successfully been extended to the description of the challenging electron distribution of systems with more complex bonding patterns, such as three-center two-electron (3c−2e) bonds in electron-deficient boron hydrides.[20] Following this line of research, our purpose is to continue studying the capability of our tools to properly describe complex structures of bonding. To this end we have chosen a class of evolving pattern boron structures,[23] the *closo*-borane family $X_2B_3H_3$ (X = BH$^-$, P, SiH, CH, N), for which classical and nonclassical alternatives of bonding have been suggested.[24,25]

The organization of this article is as follows. Section 2 briefly reports the theoretical framework of the partitioning of the electron density, the relationships between the density gradients and between the Laplacian fields, and the tools used to carry out complementary studies of topological population analysis. Section 3 describes the computational details and the discussion of the calculations performed over the selected *closo*-borane $X_2B_3H_3$ structures. Section 4 is devoted to the concluding remarks.

## 2. THEORETICAL OUTLINE

**2.1. Density Decomposition.** The electron density, $\rho(\mathbf{r})$, in an *N*-electron molecular system may be decomposed into two contributions for both closed- and open-shell state functions:[21,26]

$$\rho(\mathbf{r}) = \rho^{(p)}(\mathbf{r}) + \rho^{(u)}(\mathbf{r}) \tag{1}$$

where the effectively paired, $\rho^{(p)}(\mathbf{r})$, and unpaired, $\rho^{(u)}(\mathbf{r})$, densities are defined by

$$\rho^{(p)}(\mathbf{r}) = \frac{1}{2}\int d\mathbf{r}'\, {}^1D(\mathbf{r}|\mathbf{r}')\, {}^1D(\mathbf{r}'|\mathbf{r}) \tag{2}$$

and

$$\rho^{(u)}(\mathbf{r}) = \frac{1}{2}u(\mathbf{r}|\mathbf{r}) \tag{3}$$

respectively. ${}^1D(\mathbf{r}|\mathbf{r}')$ is the spin-free first-order reduced density matrix (1-RDM) in the coordinate representation; its trace is the number of electrons in the system, $N$.[13,14] $u(\mathbf{r}|\mathbf{r})$ is the diagonal element of the effectively unpaired density matrix defined by

$$u(\mathbf{r}|\mathbf{r}') = 2{}^1D(\mathbf{r}|\mathbf{r}') - {}^1D(\mathbf{r}|\mathbf{r}') \tag{4}$$

where ${}^1D^2(\mathbf{r}|\mathbf{r}')$ is defined by the integral in eq 2.[8−12] The densities are defined as the diagonal part of the corresponding density matrices.[13,14] The traces of the effectively paired and unpaired densities are related to the number of paired (opposite spins) and unpaired electrons under the electron correlation effects.[8,27] Two sources of unpaired density can be pointed out: one from the spin density (only present in nonsinglet states) and the other from the irreducible part or many-body cumulant of the second-order reduced density matrix (2-RDM)[20,28] being supported by the Coulomb interaction between the particles.[7,8,29] Hence, for state functions having all orbitals doubly occupied, as in the closed-shell Hartree−Fock or the density functional theory (DFT) cases, $\rho^{(u)}(\mathbf{r})$ is intrinsically zero[21] and cannot be considered for the electronic structure description of the systems.

**2.2. Electron Density Topology: Local Information.** The techniques used to study the electron density topology[17,18] can be applied to the total density and its two contributions from the above-reported partition, in order to describe the bonding features in the local frame. The localization of the cp's of each density contribution, their values, and the corresponding increment/decrease of the densities in their surroundings provide enough information to describe the electron distribution.

The cp's of the total electron density are classified regarding two values associated with the Hessian matrix of $\rho(\mathbf{r})$: its *rank r* (number of nonzero eigenvalues) and its *signature s* (sum of signs of its three eigenvalues). This information is featured as $(r,s)$. A cp with all negative eigenvalues is denoted as $(3,-3)$ and is called the nuclear critical point (ncp); it indicates a local maximum and is placed very close to the nuclear positions. A cp with two negative eigenvalues and a positive one is denoted by $(3,-1)$ and stands for a bond critical point (bcp); this type of cp corresponds to a saddle point of the electron density and denotes a bonding interaction between two atoms.[17,18] The first two eigenvalues of the Hessian matrix represent the curvatures of the densities along two axes perpendicular with respect to the third one associated with the internuclear axis. Within this framework, a covalent bond is featured by the existence of two large negative curvatures perpendicular to the bond line and a small positive curvature along the bond at the position of the bcp.[17,18] Other important cp's are the *ring* (rcp) and *cage* (ccp) critical points, which usually appear in the complex electronic structure of molecular systems; these points are characterized by rank and signature $(3,+1)$ and $(3,+3)$, respectively.[17,18] The value of $\nabla^2\rho(\mathbf{r})$ is the sum of the curvatures along the orthogonal coordinate axes; its sign indicates that the density is locally depleted (positive) or concentrated (negative)

**Table 1. Local and Integrated (Nonlocal) Topological Features of the Total Density $\rho(\mathbf{r})$ for $X_2B_3H_3$ ($X = BH^-$, P, SiH, CH, N) *closo*-Borane Systems at the CISD/6-31G** Level of Approximation[a]**

| cp type | $\rho$ sequences[b] | bond | $I_{\Omega_A\Omega_B}$ | $\Delta^{(3)}_{\Omega_A\Omega_B\Omega_C}$ |
|---|---|---|---|---|
| | **X = BH$^{-}$[c]** | | | |
| ncp | one on each B, B′, H atom | | | |
| bcp | one per each of BH bond | BB | 0.404 | |
| | one per each of B′H bond | BB′ | 0.786 | |
| | one per each of BB′ bond | BH | 0.068 | |
| | no BB bonds present | B′H | 0.681 | |
| | no B′B′ bonds present | B′B′ | 0.135 | |
| rcp | one per each BB′BB′ sequence | BBB | | 0.043 |
| ccp | one BB′BB′B | BB′B | | 0.201 |
| | | B′BB′ | | 0.000 |
| | **X = P** | | | |
| ncp | one on each P, B, H atom | | | |
| bcp | one per each of BP bond | BP | 0.853 | |
| | one per each of BH bond | BH | 0.666 | |
| | no BB bonds present | BB | 0.257 | |
| | no PP bonds present | PP | 0.317 | |
| rcp | one per each BPBP | BBB | | 0.018 |
| ccp | one PBBBP | BPB | | 0.177 |
| | | PBP | | 0.046 |
| | **X = SiH** | | | |
| ncp | one on each B, Si, H atom | | | |
| bcp | one per each of BSi bond | BSi | 0.591 | |
| | one per each of BH bond | BH | 0.782 | |
| | one per each of SiH bond | SiH | 0.590 | |
| | no BB bonds present | BB | 0.452 | |
| | no SiSi bonds present | SiSi | 0.036 | |
| rcp | one per each BSiBSi sequence | BBB | | 0.060 |
| ccp | one SiBBBSi | BSiB | | 0.121 |
| | | SiBSi | | 0.022 |
| | **X = CH** | | | |
| ncp | one on each B, C, H atom | | | |
| bcp | one per each of BC bond | BC | 0.485 | |
| | one per each of BH bond | BH | 0.547 | |
| | one per each of CH bond | CH | 1.003 | |
| | no BB bonds present | BB | 0.026 | |
| | no CC bonds present | CC | 0.697 | |
| rcp | one for each BCBCB sequence | BBB | | 0.001 |
| ccp | one CBBBC | BCB | | 0.031 |
| | | CBC | | 0.000 |
| | **X = N** | | | |
| ncp | one on each N, B, H atom | | | |
| bcp | one per each of BN bond | BN | 0.411 | |
| | one per each of BH bond | BH | 0.527 | |
| | no BB bonds present | BB | 0.017 | |
| | no NN bonds present | NN | 0.786 | |
| rcp | one per each BNBN sequence | BBB | | 0.001 |
| ccp | one NBBBN | BNB | | 0.021 |
| | | NBN | | 0.081 |

[a] All quantities are in atomic units. [b] Indicates the nucleus at which the ncp is located; for bcp's, the atoms defining the bond; for rcp's, the atoms giving rise to the ring; for ccp's, the atoms defining the cage. [c] Equatorial and vertex boron atoms are symbolized by B and B′, respectively.

and constitutes valuable information to describe the behavior of the density around a point.[17−19] According to critical point definition, the total density cp's are found by means of the

980

dx.doi.org/10.1021/ct100753q |*J. Chem. Theory Comput.* 2011, 7, 979–987

**Table 2. Local and Integrated (Nonlocal) Topological Features of the Effectively Unpaired Density $\rho^{(u)}(r)$ for $X_2B_3H_3$ (X = BH⁻, P, SiH, CH, N) *closo*-Borane Systems at the CISD/6-31G** Level of Approximation[a]**

| cp type | $\rho^{(u)}$ sequences[b] | atom | $u_{\Omega_A}$[c] |
|---|---|---|---|
| | **X = BH⁻** [d] | | |
| vs (3,−3) cp | one on each B, B′, H, H′ atom | B | 0.154 |
| | | B′ | 0.162 |
| | | H | 0.079 |
| | | H′ | 0.080 |
| vs (3,−1) cp | one per each BB′ sequence | | |
| | one per each BH and BH′ sequence | | |
| | one per each BB sequence | | |
| vs (3,+1) cp | one per each BB′B sequence | | |
| vs (3,+3) cp | one B′BBBB′ | | |
| | **X = P** | | |
| vs (3,−3) cp | one on each B, H atom | B | 0.135 |
| | one for each P atom | P | 0.304 |
| | | H | 0.073 |
| vs (3,−1) cp | one per each BP sequence | | |
| | one per each BH sequence | | |
| | one per each BB sequence | | |
| vs (3,+1) cp | one for each BPB sequence | | |
| | one BBB | | |
| vs (3,+3) cp | one for each PBBB sequence | | |
| | **X = SiH** | | |
| vs (3,−3) cp | one on each B, H atom | B | 0.200 |
| | one for each Si atom | Si | 0.108 |
| | | H (BH) | 0.075 |
| | | H (SiH) | 0.076 |
| vs (3,−1) cp | one per each BH′ sequence | | |
| | one per each BH sequence | | |
| | one per each BB sequence | | |
| vs (3,+1) cp | one per each BB sequence | | |
| | two for each BBB sequence | | |
| | one per each BH′B sequence | | |
| vs (3,+3) cp | one SiBBBBSi | | |
| | **X = CH** | | |
| vs (3,−3) cp | one on each B, H atom | B | 0.063 |
| | one for each C atom | C | 0.302 |
| | | H (BH) | 0.069 |
| | | H (CH) | 0.044 |
| vs (3,−1) cp | one per each BC sequence | | |
| | one per each BH sequence | | |
| | one per each BB sequence | | |
| vs (3,+1) cp | one for each BCB sequence | | |
| vs (3,+3) cp | one CBBBC | | |
| | **X = N** | | |
| vs (3,−3) cp | one on each B, H atom | B | 0.053 |
| | one for each N atom | N | 0.342 |
| | | H | 0.066 |
| vs (3,−1) cp | one per each BN sequence | | |
| | one per each BH sequence | | |
| | one per each BB sequence | | |
| vs (3,+1) cp | one for each BNB sequence | | |
| vs (3,+3) cp | one NBBBN | | |

[a] All quantities are in atomic units. [b] Indicates the nucleus at which the vs (3,−3) cp is located; for vs (3,−1) cp's, the atoms defining the bond; for vs (3,+1) cp's, the atoms giving rise to the ring; for vs (3,+3) cp's, the atoms defining the cage. [c] Effectively unpaired atomic electron index. [d] Equatorial and vertex borons and their linked hydrogen atoms are symbolized by B, B′ and H, H′, respectively.
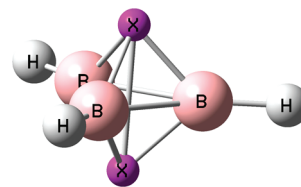


**Figure 1.** Geometric conformation of *closo*-borane systems. Atomic symbols are shown; X = BH⁻, P, SiH, CH, N.

**Table 3. Density and $L(r)$ of the Total Density $\rho$ and $\rho^{(u)}$ for $X_2B_3H_3$ (X = BH⁻, P, SiH, CH, N) *closo*-Borane Systems at Bond Critical Points of the Total Density at CISD/6-31G** Level of Calculation[a,b]**

| system[c] | bond | $\rho(r)|_{bcp}$ | $\rho^{(u)}(r)|_{bcp}$ | $-\nabla^2\rho(r)|_{bcp}$ | $-\nabla^2\rho^{(u)}(r)|_{bcp}$ | $\varepsilon$[d] |
|---|---|---|---|---|---|---|
| (B′H⁻)₂(BH)₃[e] | BB′ | 0.1354 | 0.0033 | 0.1913 | 0.0010 | 0.4210 |
| | | 0.1349 | 0.0034 | 0.2028 | 0.0012 | 0.0837 |
| | BB[f] | 0.0962 | 0.0024 | −0.0030 | −0.0014 | 0.5539 |
| | BH | 0.1482 | 0.0033 | −0.0294 | 0.0098 | 0.3686 |
| | | 0.1650 | 0.0032 | 0.4349 | 0.0043 | 0.1832 |
| | B′H | 0.1470 | 0.0033 | 0.0584 | 0.0085 | 0.0000 |
| | | 0.1640 | 0.0031 | 0.4278 | 0.0040 | 0.0000 |
| P₂(BH)₃ | BP | 0.1303 | 0.0032 | 0.1947 | 0.0125 | 0.1830 |
| | | 0.1308 | 0.0038 | 0.1942 | 0.0011 | 0.1087 |
| | BB[f] | 0.0847 | 0.0023 | −0.0130 | −0.0008 | 0.2128 |
| | BH | 0.1807 | 0.0037 | 0.2091 | 0.0117 | 0.2186 |
| | | 0.1455 | 0.0042 | −2.1590 | 0.1358 | 8.3965 |
| (SiH)₂(BH)₃ | BSi[g] | 0.1006 | 0.0023 | −0.0488 | 0.0063 | 0.3336 |
| | BB[f] | 0.0773 | 0.0021 | −0.1705 | 0.0076 | 8.1221 |
| | BH | 0.1170 | 0.0019 | −0.2584 | 0.0062 | 0.0000 |
| | | 0.1966 | 0.0035 | 0.6285 | 0.0038 | 0.1449 |
| | BH′[f] | 0.0650 | 0.0016 | 0.2483 | −0.0054 | 0.1307 |
| | SiH′[g] | 0.1170 | 0.0019 | −0.2584 | −0.0054 | 0.1307 |
| (CH)₂(BH)₃ | BC | 0.1676 | 0.0042 | −0.0582 | 0.0127 | 0.0213 |
| | | 0.1845 | 0.0039 | 0.3841 | 0.0014 | 0.0397 |
| | BB[f] | 0.0972 | 0.0230 | −0.0987 | −0.0021 | 2.0961 |
| | BH | 0.1818 | 0.0035 | 0.2050 | 0.0115 | 0.2014 |
| | | 0.1970 | 0.0032 | 0.6330 | 0.0032 | 0.1389 |
| | CH | 0.2893 | 0.0046 | 1.0788 | −0.0039 | 0.0000 |
| | | 0.2900 | 0.0045 | 1.1413 | −0.0033 | 0.0000 |
| N₂(BH)₃ | BN | 0.1924 | 0.0044 | −0.5671 | 0.0144 | 0.0490 |
| | | 0.2155 | 0.0044 | 0.3931 | 0.0047 | 0.0581 |
| | BB[f] | 0.1172 | 0.0029 | −0.1748 | −0.0008 | 1.9502 |
| | BH | 0.1894 | 0.0034 | 0.2745 | 0.0121 | 0.1229 |
| | | 0.2043 | 0.0032 | 0.6853 | 0.0026 | 0.1012 |

[a] Second row in columns 3−7 for each bond indicates the densities and $L(r)$ at $\rho^{(u)}(r)$ vs (3,−1) cp. [b] All quantities are in atomic units. [c] See Figure 1 for atom labeling. [d] Ellipticity. [e] B′, B, vertex and equatorial boron atoms, respectively. [f] There are no bcp points for $\rho(r)$ between these atoms. [g] There are no vs (3,−1) cp's for $\rho^{(u)}(r)$ between these atoms.

gradient of the field by

$$\nabla\rho(r)|_{r^c} = 0 \tag{5}$$

and according to eq 1

$$\nabla\rho^{(p)}(r)|_{r^c} + \nabla\rho^{(u)}(r)|_{r^c} = 0 \tag{6}$$

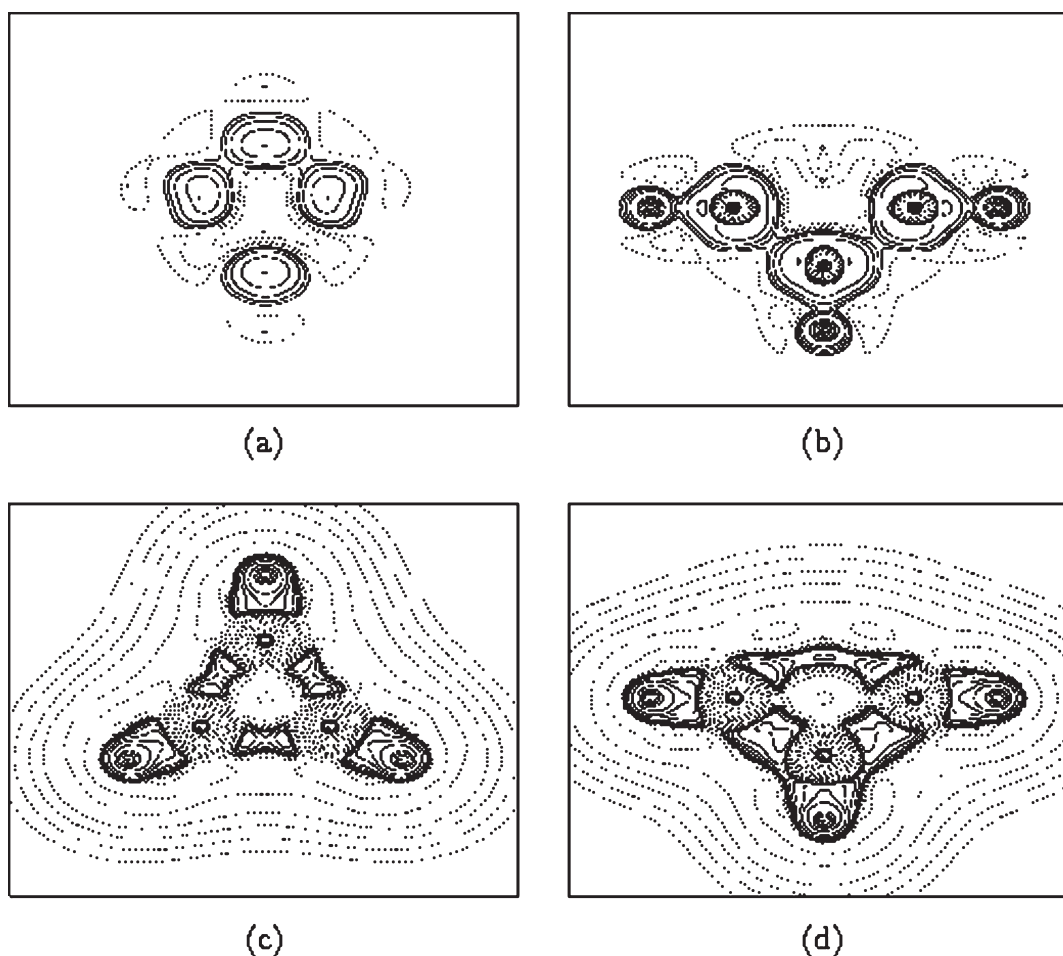where $r^c = \{r_i^c; i = 1, ..., M\}$ indicates the set of critical points of

**Figure 2.** $L(\mathbf{r})$ contour maps of effectively unpaired (a, b) and paired (c, d) densities of the $(BH^-)_2(BH)_3$ system: (a) on the plane containing two equatorial boron atoms ($B_{eq}$) and an X = B atom; (b) on the plane of the $BB_{eq}B$ atoms; (c) on the plane containing the three equatorial boron atoms ($B_{eq}$); (d) on the plane of the $BB_{eq}B$ atoms. Positive and negative values are denoted by solid and dashed lines, respectively.

the total density $\rho(\mathbf{r})$. As is obvious, the following relation holds:

$$\nabla\rho^{(p)}(\mathbf{r})|_{\mathbf{r}^c} = -\nabla\rho^{(u)}(\mathbf{r})|_{\mathbf{r}^c} \tag{7}$$

whose physical meaning is that each density field component increases/decreases its value in opposite direction. Hence, no simultaneous increment/decrease of each one may occur at the cp's.[21] Nevertheless, the Laplacian field of eq 1 yields

$$\nabla^2\rho(\mathbf{r})|_{\mathbf{r}^c} = \nabla^2\rho^{(p)}(\mathbf{r})|_{\mathbf{r}^c} + \nabla^2\rho^{(u)}(\mathbf{r})|_{\mathbf{r}^c} \neq 0 \tag{8}$$

indicating that both $\nabla^2\rho^{(p)}(\mathbf{r})|_{\mathbf{r}^c}$ and $\nabla^2\rho^{(u)}(\mathbf{r})|_{\mathbf{r}^c}$ contributions do not necessarily follow opposite trends. Hence, both densities may simultaneously concentrate or deplete in the neighborhood of a cp.[20] The terminology vs (3,−1) cp, vs (3,+1) cp, and vs (3,+3) cp will refer to (3,−1), (3,+1), and (3,+3) critical points of the $\rho^{(u)}(\mathbf{r})$ valence shell, in analogy with the bcp, rcp, and ccp's of the total density, respectively. Nevertheless, it is important to note that such points are not *sensu strictu* bcp, rcp, or ccp's because only the cp's of the total density are able to define a bond in the AIM topological formalism.[17,18]

**2.3. Electron Density Topology: Nonlocal Information.** The nonlocal or integrated formalism is complementary to the above-mentioned local one. This nonlocal formalism relates the classical chemical concepts such as atomic charges, bond orders and valences, etc. to physical magnitudes that quantify them, i.e.,

chemical indicators.[7,8,29−31] The relations defining the relevant magnitudes to our goal within the nonlocal AIM topological population analysis are the two-center bond index defined as

$$I_{\Omega_A\Omega_B} = \sum_{i,j,k,l} {}^1D_j^i\,{}^1D_l^k S_{il}(\Omega_A)\,S_{kj}(\Omega_B) \tag{9}$$

where $\Omega_A$ and $\Omega_B$ stand for Bader's atomic domains in the physical space,[17] ${}^1D_j^i$ are the first-order reduced density matrix elements, and $S_{ij}(\Omega_A)$ are the elements of the overlap matrix over the region $\Omega_A$, in the orthogonal molecular basis set $\{i, j, k, l, ...\}$,[7,29] and the three-center bond index as[30]

$$I_{\Omega_A\Omega_B\Omega_C} = \sum_{i,j,k,l,m,n} {}^1D_j^i\,{}^1D_l^k\,{}^1D_n^m S_{in}(\Omega_A)\,S_{kj}(\Omega_B)\,S_{ml}(\Omega_C) \tag{10}$$

expressing the three-center topological bonding populations by

$$\Delta^{(3)}_{\Omega_A\Omega_B\Omega_C} = \frac{1}{4}\sum_{P(\Omega_A\Omega_B\Omega_C)} I_{\Omega_A\Omega_B\Omega_C} \tag{11}$$

where $P(\Omega_A\Omega_B\Omega_C)$ indicates the permutations of the three domain contributions.

As pointed out in the Introduction, the main purpose of this paper is to study the capability of these tools to describe
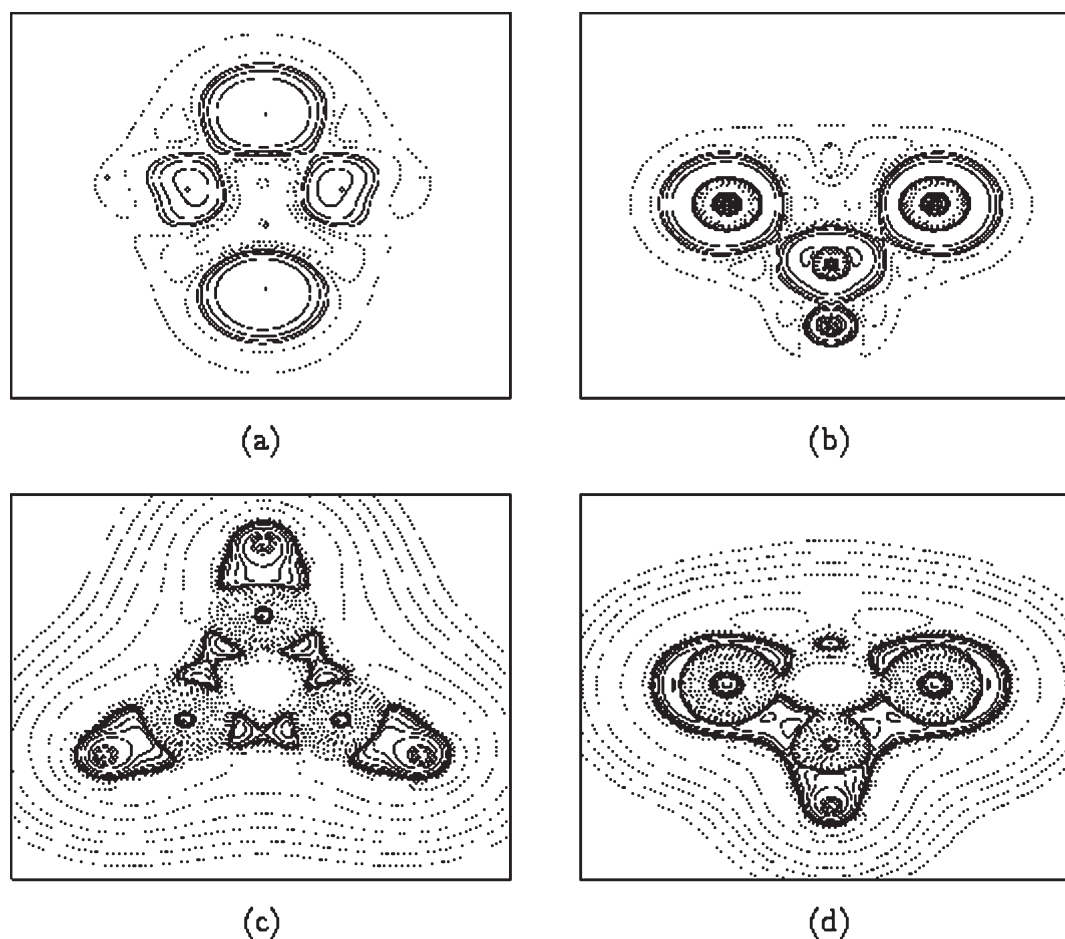
**Figure 3.** $L(\mathbf{r})$ contour maps of effectively unpaired (a, b) and paired (c, d) densities of the $P_2(BH)_3$ system: (a) on the plane containing two equatorial boron atoms ($B_{eq}$) and an X = P atom; (b) on the plane of the $PB_{eq}P$ atoms; (c) on the plane containing the three equatorial boron atoms ($B_{eq}$); (d) on the plane of the $PB_{eq}P$ atoms. Positive and negative values are denoted by solid and dashed lines, respectively.

nonclassical patterns of bonding such as the 3c—2e, among others. The results are reported in section 3.

## 3. COMPUTATIONAL DETAILS, RESULTS, AND DISCUSSION

As is well-known, the boron atom forms electron-deficient compounds giving rise to 3c—2e bonds in boron hydrides.[23] A previous study permitted noting that the onset of such a bonding character seems to be closely related to the effectively unpaired electron density distribution featured by the unpaired electron delocalization on the bonding regions, its accumulation on the bcp's, and the existence of vs $(3,-1)$ cp's and vs $(3,+1)$ cp's of $\rho^{(u)}(\mathbf{r})$ between the atoms involved.[26] Therefore, the next step is to search for applications that would reveal the physical meaning of these characteristics in more complex structures. To this end, we have chosen a family of boron compounds, i.e., the *closo*-borane clusters $X_2B_3H_3$ (X = N, CH, P, $BH^-$, SiH),[23,24] which incorporate a new feature, i.e., additional electrons provided by the X group. These types of systems are natural candidates to possess 3c—2e patterns of bonding. Hence, this scenario is adequate to enlighten the nature of this pattern passing from typical boron hydrides to more complex borane systems which seem to have nonclassical bonding structures.[24]

The state functions used in this work to describe the selected molecular systems in their singlet ground states were calculated at the level of configuration interaction with single and double excitations (CISD) and the singlet RHF state as reference, using the Gaussian 03 package[32] with the basis sets 6-31G**. The geometries for all systems were optimized within this approximation. The densities, their critical points, and their Laplacian fields $\nabla^2\rho(\mathbf{r})$ and $\nabla^2\rho^{(u)}(\mathbf{r})$ were determined by appropriately modified AIMPAC modules.[33] The numerical results of the electron population analysis were obtained with our own codes.[30] For practical reasons, we will use the function $L(\mathbf{r}) = -\nabla^2\rho(\mathbf{r})$ in the discussion of results as an indicator of local concentration (positive value) or local depletion (negative value) of the number of electrons at the point $\mathbf{r}$;[20–22,26] the terms "accumulation" and "reduction" have been proposed for the description of maxima and minima in $\rho(\mathbf{r})$.[18,35] Because of the complex structure of the $\rho^{(u)}(\mathbf{r})$ topology, we will only deal in our study with critical points associated with its valence shells (vs) in the corresponding systems and no reference will be made to those of the inner shells of this density; in fact, only the former ones are involved in bonding phenomena.

Before discussing the results, let us enunciate the previously establish quantum based rule to detect 3c—2e bonds in borane clusters to be applied to the complex structure of *closo*-borane
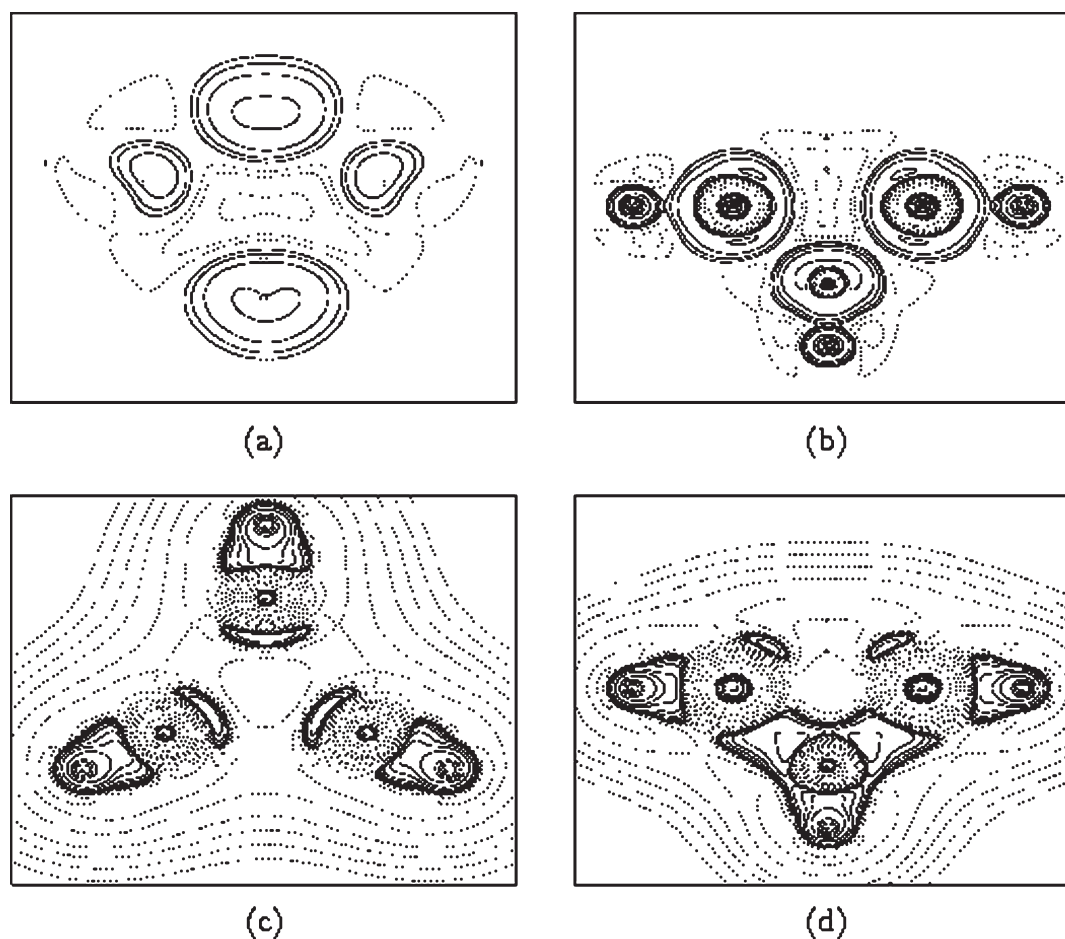
983

dx.doi.org/10.1021/ct100753q |*J. Chem. Theory Comput.* 2011, 7, 979–987

**Figure 4.** $L(\mathbf{r})$ contour maps of effectively unpaired (a, b) and paired (c, d) densities of the $(SiH)_2(BH)_3$ system: (a) on the plane containing two equatorial boron atoms ($B_{eq}$) and an X = Si atom; (b) on the plane of the $SiB_{eq}Si$ atoms; (c) on the plane containing the three equatorial boron atoms ($B_{eq}$); (d) on the plane of the $SiB_{eq}Si$ atoms. Positive and negative values are denoted by solid and dashed lines, respectively.

molecular systems, in a general manner as follows: *a 3c−2e bond between atoms ABC exists if there is a vs (3,−1) cp of $\rho^{(u)}$ between each pair of atoms involved in the three-center ABC sequence and a vs (3,+1) cp defined only by the atoms involved in the three-center bond*, hereafter called the *local rule*.[20] This result seems to be the local version of the criterion of the integrated formalism of population analysis for detecting three-center bonding, hereafter the *integrated* or *nonlocal rule*. That criterion settles the existence of a 3c−2e bond between atoms ABC when fractional bond orders $I_{\Omega_A\Omega_B}$ appear between all possible pairs of atoms AB, BC, and AC and an appreciable $\Delta_{\Omega_A\Omega_B\Omega_C}^{(3)}$ defines its strength.[4,36] Because of the detailed description of the distribution from the topological (local) view, we will adopt this form of the rule as the indicator of the quality of the interaction between the atoms while the integrated form is interpreted as an indicator of the strength of such interaction; i.e., the local rule defines the existence of such a type of interaction between the atoms while the integrated (nonlocal) form of the rule adjudicates the strength of the interaction by means of the population shared by the atoms involved.

Figure 1 shows the geometric conformation of the *closo*-borane cluster compounds $X_2B_3H_3$ (X = N, CH, P, BH⁻, SiH).[23−25,34] Three boron atoms are located at the equatorial plane, each one bonded to a hydrogen atom. The X vertex moieties are symmetrically placed above and below the

equatorial plane.[23] Table 1 contains the topological information concerning the total density $\rho(\mathbf{r})$, showing the localization of the cp's, their type and the atomic sequence which defines each of them, the two-center bond indices $I_{\Omega_A\Omega_B}$, and the three-center bonding electron populations $\Delta_{\Omega_A\Omega_B\Omega_C}^{(3)}$. Table 2 is devoted to the topological structure of $\rho^{(u)}(\mathbf{r})$ and the number of effectively unpaired electron $u_{\Omega_A}$ values. Note that no reference to the effectively paired density $\rho^{(p)}(\mathbf{r})$ is made in Table 2 because as shown in previous articles, its structure is similar to that of $\rho(\mathbf{r})$ and therefore it does not introduce any new information.[21,22]

As mentioned above, Table 1 summarizes the main parameters describing the structure of the systems. It reports the nonnegligible values of the two-center covalent bond indices $I_{\Omega_A\Omega_B}$ and the three-center populations $\Delta_{\Omega_A\Omega_B\Omega_C}^{(3)}$. The information contained in Table 1 indicates that the boron atoms in the equatorial plane of the molecules are not bonded to each other, i. e., there is no bcp defined by two of them in any of these systems. However, they are bonded to the heavy atom in the X moieties. Nonnegligible two-center indices are obtained between the heavy atom of both X groups for $X_2B_3H_3$, X = CH, N (approximately 0.7 and 0.8, respectively); however, no bonding character appears because there is no bcp defined between them. This means that the electron density accumulates in a spatial region between these atoms but it does not constitute a bond. Such an amazing feature will be discussed in more detail later. An
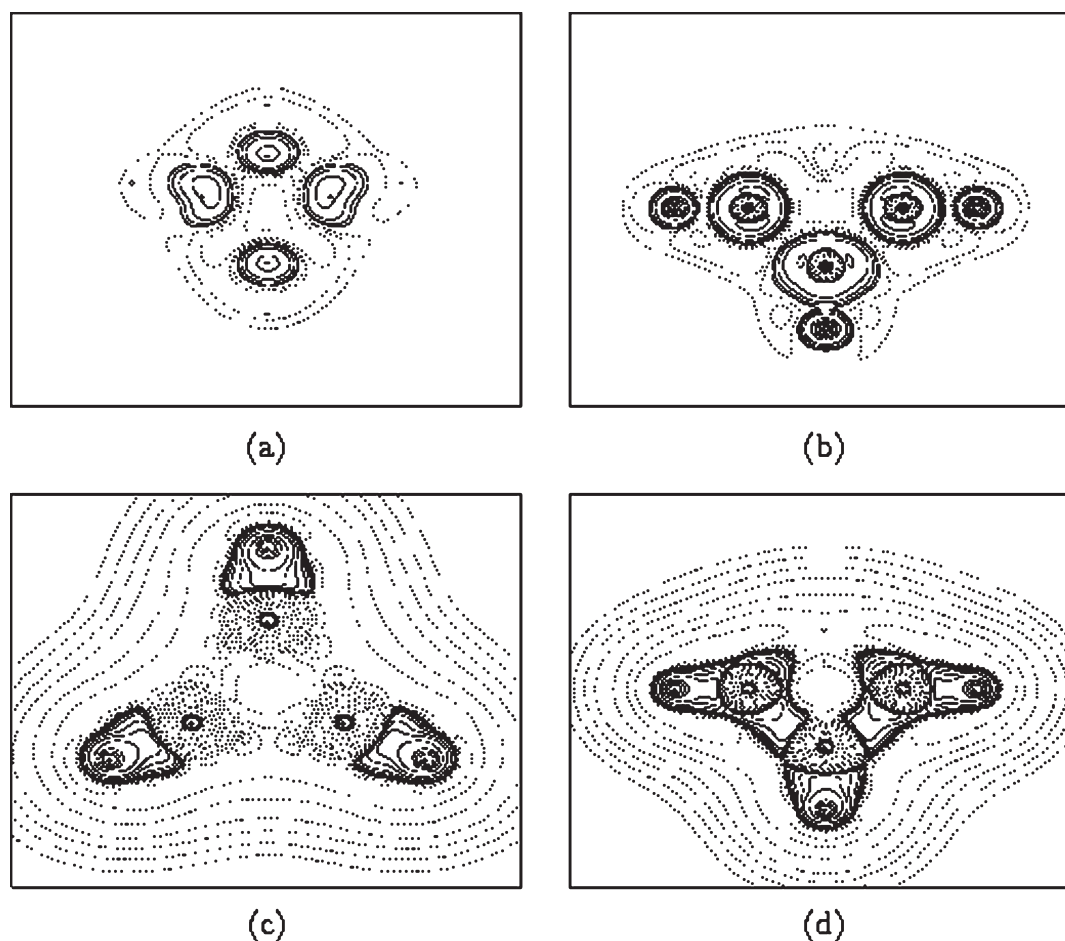
**Figure 5.** $L(\mathbf{r})$ contour maps of effectively unpaired (a, b) and paired (c, d) densities of the $(CH)_2(BH)_3$ system: (a) on the plane containing two equatorial boron atoms ($B_{eq}$) and an X = C atom; (b) on the plane of the $CB_{eq}C$ atoms; (c) on the plane containing the three equatorial boron atoms ($B_{eq}$); (d) on the plane of the $CB_{eq}C$ atoms. Positive and negative values are denoted by solid and dashed lines, respectively.

rcp for each sequence formed by two of the equatorial boron atoms and the heavy atom of both X moieties is present in the systems. All the systems possess one ccp formed by these two atoms and the three equatorial boron atoms. Regarding the three-center populations, we may note that the BBB equatorial sequence shows low values indicating a small shared population of 0.043, 0.018, and 0.060 for X = $BH^-$, P, and SiH, respectively, and a negligible one for X = CH and N. However, the sequence BXB shows such a type of bonding population increasing from 0.021 to 0.201 according to N < CH < SiH < P < $BH^-$. Some of the systems also show XBX nonnegligible populations, indicating weak 3c–2e bonds for X = P, SiH, and N. The cases of X = $BH^-$ and CH do not show this bonding character.

Table 2 collects the information from $\rho^{(u)}(\mathbf{r})$ required to apply the local form of the rule to detect 3c–2e bonds.[20] Hence, following this rule, all systems except X = SiH possess 3c–2e bonds formed by the heavy atom of the X moiety and two equatorial boron atoms, i.e., BXB; the strength of each of these bonds is stated by the corresponding three-center population collected in Table 1, as reported above. The unpaired electron distribution around the *Si* atom is particularly complex, and it is not possible to assign a vs (3,−1) cp to the BX interactions in this case. However, the appearance of a vs (3,−1) cp for the sequences BB and BH′ (where H′ represents the hydrogen atom in the X = SiH moiety) and a vs (3,+1) cp for each BH′B

sequence may be noted. These last features could explain the 0.121 three-center population reported in Table 1 for the BSiB sequence of this complex system. The observation of the increment of the $u_\Omega$ populations of the boron atoms in the equatorial plane following the sequence N < CH < P < $BH^-$ < SiH and a corresponding decrease of that of X's (see Table 2) may be interpreted as a transference of unpaired electron population from the three equatorial boron atoms toward the heavy atoms in the X moieties in all systems considered.

Table 3 and Figures 2–6 permit completion of the description of the above featured behavior of the electron distribution in the reported systems. Table 3 collects the values of the total and the unpaired densities and their associated Laplacian fields at the neighborhoods of the bcp's and vs (3,−1) cp's. Figures 2a,b–6a, b show the unpaired density maps on the planes defined by two equatorial boron atoms and the heavy atom of the X moiety and on the plane defined by the heavy atom in both X moieties and an equatorial boron atom, respectively. The paired density maps are shown on the equatorial plane in Figures 2c–6c, and Figures 2d–6d show this density at the same plane as Figures 2b–6b. The sign of the $L(\mathbf{r})$ function in Table 3 reveals concentration of both total and unpaired densities at the BX bcp and the vs (3,−1) cp for the X = $BH^-$, P systems; Figures 2a,b and 3a,b show that such concentration of $\rho^{(u)}(\mathbf{r})$ spills on the internuclear bonding spatial regions of these systems, as previously
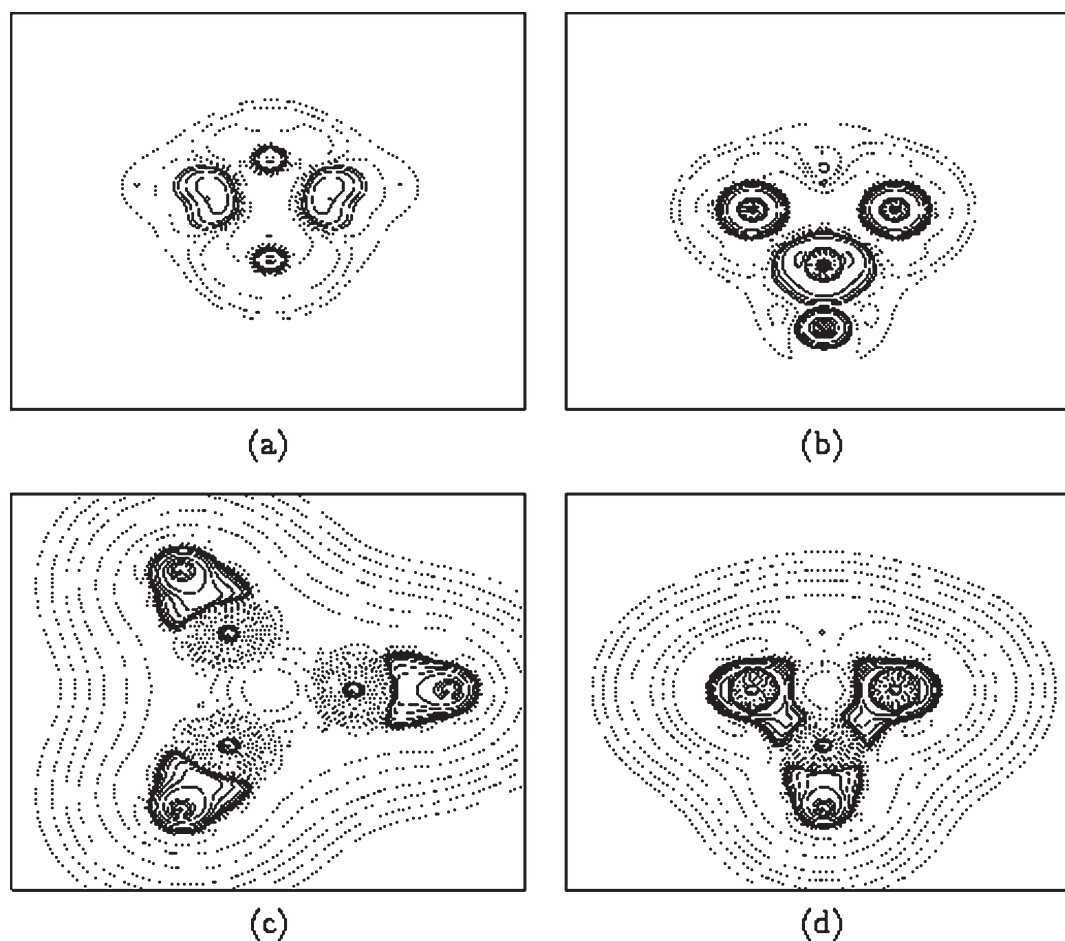
**Figure 6.** $L(\mathbf{r})$ contour maps of effectively unpaired (a, b) and paired (c, d) densities of the $N_2(BH)_3$ system: (a) on the plane containing two equatorial boron atoms ($B_{eq}$) and an $X = N$ atom; (b) on the plane of the $NB_{eq}N$ atoms; (c) on the plane containing the three equatorial boron atoms ($B_{eq}$); (d) on the plane of the $NB_{eq}N$ atoms. Positive and negative values are denoted by solid and dashed lines, respectively.

noted for boron hydrides.[20] The remaining systems, X = SiH, CH, and N, show marked depletion of $\rho(\mathbf{r})$ at the BX bcp, while $\rho^{(u)}(\mathbf{r})$ remains concentrated at the vs $(3,-1)$ cp's (cf. Table 3); i.e., there is an important shift of the bcp and vs $(3,-1)$ cp; Figures 4a,b, 5a,b, and 6a,b complement this result showing the unpaired density depletion in the spatial region between the above-mentioned atoms and its accumulation close to the nuclear positions. Hence, $\rho^{(u)}(\mathbf{r})$ becomes accumulated in all systems at bcp's, while $\rho(\mathbf{r})$ does not. This behavior may not show either ionic or covalent trends,[22] which indicates a more complex type of bonding as described previously for boron hydrides.[20]

The results described above evidence the presence of complex patterns of bonding, i.e., the existence of 3c–2e bonds defined by the BXB atoms. However, there is no evidence of 3c–2e BBB bonds. These reasons lead to consideration of nonclassical patterns of bonding for the electronic structure of all systems treated in this work (cf. ref 24). An important feature within these nonclassical structures that deserves discussion to complete the understanding of the electronic structure of these systems is related to the high value of some covalent two-center bond indices, i.e., between two equatorial boron atoms or between two heavy atoms, one on each X moiety, despite no bcp defining a true bond between them. This may be considered as a feature of the electron distribution that relates to some extent the nonlocal

and the local formulations of description. Let us begin with the first of the mentioned sequences, that is, the BB equatorial boron atoms. The $I_{\Omega_B \Omega_B}$ value increases following the N < CH < P < BH$^-$ < SiH ordering. To explain this behavior, we may note the contour maps of the $L(\mathbf{r})$ function of the effectively paired densities on the equatorial plane of the molecule (Figures 2c–6c), bearing in mind that integration of this density inside the corresponding atomic basins determines the two-center index (cf. eq 9). The systems with X = SiH, BH$^-$, and P moieties have appreciable values of 0.452, 0.404, and 0.257, respectively, for these $I_{\Omega_B \Omega_B}$ indices, in agreement with the pair density accumulation in the internuclear regions shown in Figures 2c–6c. Very small bond indices of 0.026 and 0.017 for X = CH and N, respectively, are due to the marked depletion of the density in the mentioned regions. A similar analysis may be performed for the bondings between the heavy atoms of the X moieties, graphically shown in Figures 2d–6d. Finally, it is worth noting the relation between the covalent bond indices $I_{\Omega_B \Omega_B}$ and $I_{\Omega_X \Omega_X}$. It may be noted that $I_{\Omega_B \Omega_B}$ increases from 0.017 to 0.452 following the sequence mentioned above, while $I_{\Omega_X \Omega_X}$ decreases following the inverse sequence from 0.786 to 0.036. Therefore, the equatorial boron atom bonding populations decrease according to the increase of the bonding electron population of the heavy atom in the X moiety, in agreement with the increase of its electronegativity.

## 4. CONCLUDING REMARKS

It is well-known that B atoms tend to form electron-deficient compounds, particularly in boron hydrides. In this work, we have dealt with *closo*-borane molecular systems, where additional electrons are available and therefore such electron deficiency is broken. Our main goal has been to characterize and to test our previously stated rule to detect and describe systems possessing 3c−2e complex patterns of bonding. From the present study we may conclude that the topological description of the local rule has been successfully applied to these type of systems and its nonlocal counterpart acts as an indicator of the strength of this interaction. Although the systems are not electron deficient, $\rho^{(u)}(\mathbf{r})$ remains spilled on the spatial bonding regions as noted previously in boron hydrides. Besides, it may be pointed out that the only knowledge of the total density does not provide a complete description of the electron structure of these type of systems. Therefore, the topology of $\rho^{(u)}(\mathbf{r})$ supplies some new type of information regarding the structure of the electron distributions of complex systems.

A result dealing with the strength of the covalent bond order $I_{\Omega_A\Omega_B}$ and the existence of a bond critical point bcp which defines the linkage between atoms in the molecule may be remarked: an appreciable $I_{\Omega_A\Omega_B}$ does not always imply the existence of a true bond (for instance $I_{\Omega_N\Omega_N} = 0.786$ in $N_2B_3H_3$ but there is no bcp between two atoms). This is an amazing result that merits a further detailed study on systems with complex patterns of bonding. Extensions of this type of analysis which exploits the information contained in $\rho^{(u)}(\mathbf{r})$ to understand other complex bonding systems such as organometallic and hydrogen bonded compounds are being considered in our laboratories.

## ■ AUTHOR INFORMATION

**Corresponding Author**
*E-mail: rboc@df.uba.ar.

## ■ ACKNOWLEDGMENT

## ■ REFERENCES

(1) Giambiagi, M.; Giambiagi, M. S.; Grempel, D. R.; Heymann, C. D. *J. Chim. Phys.* **1975**, *72*, 15.

(2) Mayer, I. *Chem. Phys. Lett.* **1983**, *97*, 270.

(3) Mayer, I. *Int. J. Quantum Chem.* **1986**, *29*, 73.

(4) Bochicchio, R. C. *THEOCHEM* **1991**, *228*, 209 and references therein.

(5) Bochicchio, R. C.; Lain, L.; Torre, A. *Chem. Phys. Lett.* **2003**, *374*, 567 and references therein.

(6) Alcoba, D. R.; Bochicchio, R. C.; Lain, L.; Torre, A. *Chem. Phys. Lett.* **2007**, *442*, 157.

(7) Bochicchio, R. C.; Lain, L.; Torre, A. *Chem. Phys. Lett.* **2003**, *375*, 45.

(8) Bochicchio, R. C. *THEOCHEM* **1998**, *429*, 229.

(9) Lain, L.; Torre, A.; Bochicchio, R. C.; Ponec, R. *Chem. Phys. Lett.* **2001**, *346*, 283.

(10) Takatsuka, K.; Fueno, T.; Yamaguchi, K. *Theor. Chim. Acta* **1978**, *48*, 175.

(11) Takatsuka, K.; Fueno, T. *J. Chem. Phys.* **1978**, *69*, 661.

(12) Staroverov, V. N.; Davidson, E. R. *Chem. Phys. Lett.* **2000**, *330*, 161.

(13) McWeeny, R. *Methods of Molecular Quantum Mechanics*; Academic: London, 1969; pp 115−158 and references therein.

(14) Davidson, E. R. *Reduced Density Matrices in Quantum Chemistry*; Academic: New York, 1976; pp 57−96 and references therein.

(15) Bamzai, A. S.; Deb, B. M. *Rev. Mod. Phys.* **1981**, *53*, 95.

(16) Szabo, A.; Ostlund, N. S. *Modern Quantum Chemistry: Introduction to Advanced Electronic Structure*; Macmillan: New York, 1982; pp 203−205 and references therein.

(17) Bader, R. F. W. *Atoms in Molecules: A Quantum Theory*; Clarendon Press: Oxford, U.K., 1994; pp 13−52 and references therein.

(18) Popelier, P. L. A. *Atoms in Molecules: An Introduction*; Pearson: London, 1999; pp 70−80.

(19) Bader, R. F. W. *Chem.—Eur. J.* **2006**, *12*, 7769.

(20) Lobayan, R. M.; Bochicchio, R. C.; Torre, A.; Lain, L. *J. Chem. Theory Comput.* **2009**, *5*, 2030 and references therein.

(21) Lobayan, R. M.; Bochicchio, R. C.; Lain, L.; Torre, A. *J. Chem. Phys.* **2005**, *123*, 144116.

(22) Lobayan, R. M.; Bochicchio, R. C.; Lain, L.; Torre, A. *J. Phys. Chem. A* **2007**, *111*, 3166.

(23) Fox, M. A.; Wade, K. *Pure Appl. Chem.* **2003**, *75*, 1315 and references therein.

(24) von Ragué Schleyer, P.; Subramanian, G.; Dransfeld, A. *J. Am. Chem. Soc.* **1996**, *118*, 9988.

(25) Torre, A.; Lain, L.; Bochicchio, R.; Ponec, R. *J. Comput. Chem.* **1999**, *20*, 1085.

(26) Lobayan, R. M.; Alcoba, D. R.; Bochicchio, R. C.; Torre, A.; Lain, L. *J. Phys. Chem. A* **2010**, *114*, 1200.

(27) Luzanov, A. V.; Prezhdo, O. V. *Mol. Phys.* **2007**, *105*, 2879.

(28) Lain, L.; Torre, A.; Alcoba, D. R.; Bochicchio, R. C. *Chem. Phys. Lett.* **2009**, *476*, 101.

(29) Torre, A.; Lain, L.; Bochicchio, R. *J. Phys. Chem. A* **2003**, *107*, 127.

(30) Lain, L.; Torre, A.; Bochicchio, R. *J. Phys. Chem. A* **2004**, *108*, 4132.

(31) Cioslowski, J.; Mixon, S. T. *J. Am. Chem. Soc.* **1991**, *113*, 4142.

(32) Frisch, M. J.; Trucks, G. W.; Schlegel, H. B.; Scuseria, G. E.; Robb, M. A.; Cheeseman, J. R.; Montgomery, J. A., Jr.; Vreven, T.; Kudin, K. N.; Burant, J. C.; Millam, J. M.; Iyengar, S. S.; Tomasi, J.; Barone, V.; Mennucci, B.; Cossi, M.; Scalmani, G.; Rega, N.; Petersson, G. A.; Nakatsuji, H.; Hada, M.; Ehara, M.; Toyota, K.; Fukuda, R.; Hasegawa, J.; Ishida, M.; Nakajima, T.; Honda, Y.; Kitao, O.; Nakai, H.; Klene, M.; Li, X.; Knox, J. E.; Hratchian, H. P.; Cross, J. B.; Adamo, C.; Jaramillo, J.; Gomperts, R.; Stratmann, R. E.; Yazyev, O.; Austin, A. J.; Cammi, R.; Pomelli, C.; Ochterski, J. W.; Ayala, P. Y.; Morokuma, K.; Voth, G. A.; Salvador, P.; Dannenberg, J. J.; Zakrzewski, V. G.; Dapprich, S.; Daniels, A. D.; Strain, M. C.; Farkas, O.; Malick, D. K.; Rabuck, A. D.; Raghavachari, K.; Foresman, J. B.; Ortiz, J. V.; Cui, Q.; Baboul, A. G.; Clifford, S.; Cioslowski, J.; Stefanov, B. B.; Liu, G.; Liashenko, A.; Piskorz, P.; Komaromi, I.; Martin, R. L.; Fox, D. J.; Keith, T.; Al-Laham, M. A.; Peng, C. Y.; Nanayakkara, A.; Challacombe, M.; Gill, P. M. W.; Johnson, B.; Chen, W.; Wong, M. W.; Gonzalez, C.; Pople, J. A. *Gaussian 03*, revision C.02; Gaussian, Inc.: Wallingford, CT, USA, 2004.

(33) Biegler-Köning, F. W.; Bader, R. F. W.; Tang, T. H. *J. Comput. Chem.* **1982**, *3*, 317.

(34) Wade, K. *Nat. Chem.* **2009**, *1*, 92.

(35) Popelier, P. L. A. *Coord. Chem. Rev.* **2000**, *197*, 169.

(36) Bochicchio, R.; Ponec, R.; Uhlik, P. *Inorg. Chem.* **1997**, *36*, 5363 and references therein.

987

dx.doi.org/10.1021/ct100753q |*J. Chem. Theory Comput.* 2011, 7, 979–987